Hydrostatic pressure dependence of indirect and direct excitons in InGaN/GaN quantum wells

G. Staszczak,[1] W. Trzeciakowski,[1] E. Monroy,[2] A. Bercha,[1] G. Muzioł,[1] C. Skierbiszewski,[1,3] P. Perlin,[1,3] and T. Suski[1]

[1]*Institute of High Pressure Physics, Polish Academy of Sciences, Sokołowska 29/37, 01-142 Warsaw, Poland*
[2]*Univ. Grenoble-Alpes, CEA, IRIG-PHELIQS, 17 Avenue des Martyrs, 38000 Grenoble, France*
[3]*TopGaN, Sokolowska 29-37, PL-01142 Warsaw, Poland*

(Received 16 July 2019; revised manuscript received 28 November 2019; accepted 10 February 2020; published 28 February 2020)

We analyze the evolution of the exciton recombination energy E_{PL} and its pressure coefficient dE_{PL}/dp, with the laser power density (LPD) exciting excitonic photoluminescence. Two $In_{0.17}Ga_{0.83}N/GaN$ quantum well (QW) structures are used: sample A consisting of a 5.2-nm-wide single QW and sample B consisting of two 2.6-nm-wide QWs separated by a 0.78-nm-thick barrier. Changes of E_{PL} and dE_{PL}/dp with LPD in both structures cover a wide range of magnitude. They switch character in the vicinity of the indirect to direct exciton induced by increasing LPD. In sample B, at low excitation, a negative pressure coefficient of E_{PL} has been found. Moreover, pressure dependences of E_{PL} are different for the two samples under study. We examined pressure dependence of the threshold LPD for indirect-direct exciton switching in both samples. The reported observations originate to a high extent from screening of a built-in electric field by carriers externally introduced into the quantum wells. We also note that the universal relation between transition energies and their pressure coefficients (observed previously in InGaN/GaN quantum wells) does not hold for samples modified by screening.

DOI: 10.1103/PhysRevB.101.085306

I. INTRODUCTION

Optoelectronic devices based on polar heterostructures of nitride semiconductors (InGaN/GaN, GaN/AlGaN, AlInN/GaN) demonstrate high quantum efficiency, which generated many applications including general lighting and displays [1–5]. The strong built-in electric fields arising from the spontaneous and piezoelectric polarization represent a key issue in the design of the active region of these devices [6–9]. The most important consequences of the presence of the internal electric field in III-nitride quantum structures are described by the quantum confined Stark effect (QCSE). The QCSE leads to tilted band profiles, spatial separation of electron- and hole-wave functions, and a strong redshift of the light emission energy. Polar heterostructures of nitride semiconductors display internal electric fields exceeding 1 MV/cm and approaching sometimes even 10 MV/cm [6,7,10,11]. This built-in electric field is detrimental in optoelectronic devices such as light emitting diodes (LEDs) and laser diodes (LDs).

According to predictions of QCSE, structures with wider quantum wells (QWs) exhibit more pronounced effects of the internal electric field. It has been demonstrated very recently that the redshift of the photoluminescence (PL) measured in wide QWs of $In_{0.17}Ga_{0.83}N/GaN$ can approach 0.5 eV [8]. Screening of the internal electric field by means of high-power-density laser excitation leads to the large (almost entire) reduction of the QCSE, up to the saturation of the blueshift of the exciton recombination energy [Fig. 1(a)].

For $In_{0.17}Ga_{0.83}N/GaN$ structures consisting of double QWs separated by a narrow barrier [Fig. 1(b)], the presence of electric field F_{int} causes the formation of indirect, interwell excitons (IXs) [8]. With increasing laser power density (LPD), the PL peak energy E_{PL} shows a strong blueshift and eventually (after sufficient screening of electric field F_{int}) excitons change their character to direct, intrawell excitons (DXs). Once the DX is formed [right panels in Figs. 1(a) and 1(b)], it exhibits very limited blueshift of the PL energy with increasing LPD [8]. Increasing the interwell barrier width from 0.5 to 2 nm shifts the LPD threshold that marks the transition from IX to DX to lower LPD values [8]. This demonstrates the role of exciton/carrier tunneling involved in the formation of IXs. Barriers narrower than 0.5 nm are not seen by excitons and, as a result, the IX-DX switching is similar as in QW structures without a barrier [Figs. 1(a) and 2(a)].

The terminology IX and DX which we use in the present paper requires some explanation. In double QWs with a wide barrier the distinction between two types of excitons is rather clear, namely, IX describes the interwell exciton and DX refers to intrawell exciton. However, for very thin barriers or for a vanishing barrier the continuous evolution of the states shown in Fig. 1 does not allow for a clear distinction. We still use these two terms based on the experimentally observed dependence of the E_{PL} on LPD. Thus, for indirect excitons E_{PL} increases strongly with LPD while for direct excitons E_{PL} changes slowly with LPD [10].

For the three last decades, indirect excitons in GaAs/AlGaAs double QWs subjected to an external electric field have been analyzed intensively [9,12,13]. Exciting issues like Bose-Einstein condensation of indirect excitons [14–16] and the design of excitonic devices [17–19] are highly cited results of these studies. More recently, IXs in wide (6–8 nm) single QWs of GaN/AlGaN have been reported, including

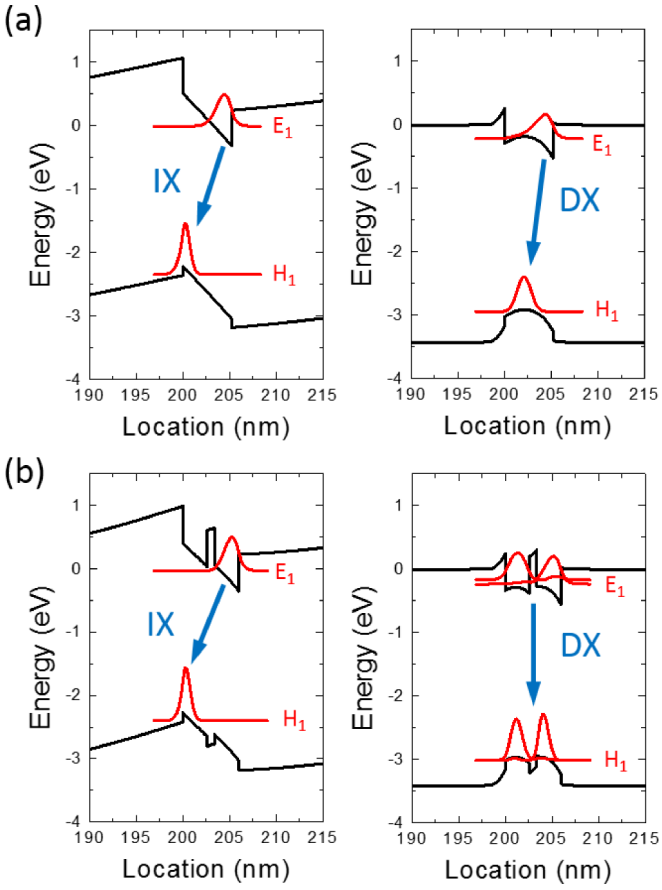

FIG. 1. Schematic illustration of changes in the band profile (screening) for low LPD (left-hand side) and for high LPD (right-hand side) (a) in a single, wide $In_{0.17}Ga_{0.83}N/GaN$ quantum well, and (b) in a double $In_{0.17}Ga_{0.83}N/GaN$ quantum well with a narrow barrier. The built-in (internal) electric field in the studied samples is strongly reduced by pumping excitons/carriers into quantum wells. E_1 and H_1 represent ground states of electrons and holes. IX and DX denote indirect and direct excitons, respectively.

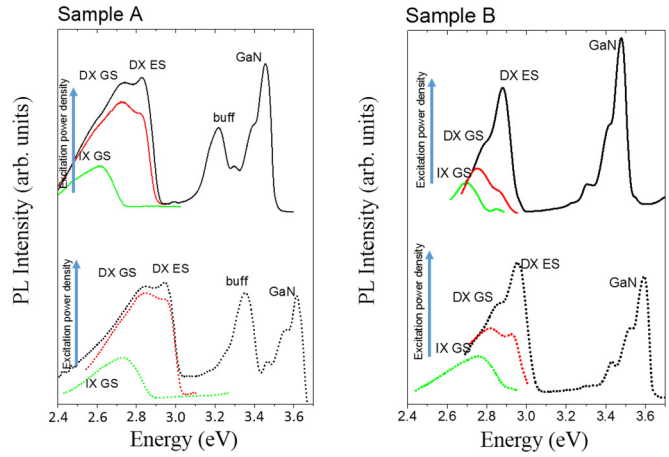

FIG. 2. Evolution of the PL spectra at low pressure (upper part of the figures) and at high pressure (lower part of the figures) for three different magnitudes of the exciting laser power. Left (right) part of diagrams shows results obtained for sample A (sample B). The labels "IX GS," "DX GS," and "DX ES" refer to indirect exciton, direct exciton ground state, and direct exciton excited state, respectively.

also demonstrations of their lateral transport over large distances [20,21].

Heterostructures of III-N semiconductors seem to be more attractive than arsenides in terms of exciton stability. The binding energy of excitons in GaAs is about 3 meV, whereas for InN, GaN, and AlN binary compounds it is about 20, 30, and 60–70 meV, respectively [22]. Therefore, due to the large exciton binding energy, heterostructures such as GaN/AlGaN and InGaN/GaN are much more suitable candidates than arsenide QWs for the study of IXs. Excitons in nitride QWs can be stable over a wide temperature range (even > 100 K), when created by excitation with a moderate laser power [23].

Effects of the internal electric field have been studied recently in InGaN/GaN QWs by application of hydrostatic pressure [24–26]. Previous pressure-dependent studies have shown that in nonpolar nitride heterostructures [27] and in cubic QWs of other semiconductor systems, e.g., GaAs/AlGaAs [28], the shift of the PL peak energy reflects an increase of the band gap of the QW material with applied pressure. On the contrary, in the case of polar InGaN/GaN, GaN/AlGaN, and GaN/AlInN heterostructures, the existing results [24–26] revealed a strong contribution of the pressure-induced increase of the built-in field in the QW (F_{int}), which results in a reduction of the pressure coefficient of the transition energy by an amount proportional to the QW width $\times F_{\text{int}}$ product. Another interesting observation was a "universal" linear dependence between E_{PL} and its pressure coefficients dE_{PL}/dp [25,26]. "Universal" meant that, in $In_xGa_{1-x}N$ wells, this relation was independent of the well width L and composition x. As shown in Ref. [26] the physical reason for the independence of L is the fact that the confinement energy does not depend on L in wells with high internal electric fields. The calculated energies and their pressure coefficients were still dependent on L, but the relationship between them no longer contained L.

Both effects described above demonstrate the specific role of a built-in electric field in the determination of optical properties in nitride heterostructures.

There were two interrelated purposes of this work. The first target was to compare an evolution of E_{PL} and dE_{PL}/dp with the LPD in two samples consisting of a single InGaN/GaN QW and a double InGaN/GaN QW with a very thin interwell barrier, but keeping total InGaN width the same in both samples. The second goal was to verify the above-mentioned universal linear dependence between E_{PL} and dE_{PL}/dp in the case of electric field modification by the LPD, i.e., to check how the changes of E_{PL} correlate with the changes of dE_{PL}/dp when both are caused by the LPD.

II. SAMPLES AND EXPERIMENT

PL studies under pressure have been performed for two InGaN/GaN samples with different structures grown by plasma-assisted molecular beam epitaxy. They were deposited on bulk GaN substrates with a 2-μm-thick GaN:Si buffer layer and a 20-nm-thick $In_{0.02}Ga_{0.98}N$ barrier layer. Investigated samples consist of either single or double $In_{0.17}Ga_{0.83}N$ QWs. Sample A consists of a single 5.2-nm-wide QW while sample

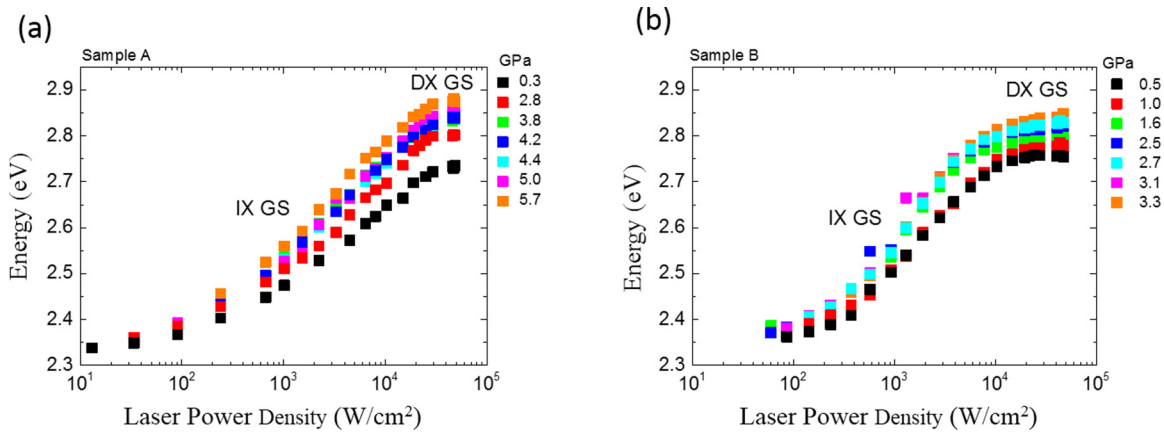

FIG. 3. PL peak energy of excitons versus the power density of the exciting laser for (a) samples A and (b) sample B. Different colors correspond to different values of hydrostatic pressure applied to the samples. For sample A, higher pressure leads to higher transition energies. For sample B, a more complex trend is observed.

B contains two 2.6-nm-wide QWs separated by a 0.78-nm-thick $In_{0.02}Ga_{0.98}N$ quantum barrier (QB). Both samples were capped by 20-nm-thick, undoped $In_{0.02}Ga_{0.98}N$ barriers. In comparison to GaN barriers, structures with a small amount of indium in the barriers have much higher structural quality of interfaces between barriers and QWs.

The samples were previously analyzed by high-resolution x-ray diffraction (XRD), transmission electron microscopy (TEM), continuous-wave photoluminescence (PL), and time-resolved photoluminescence (TRPL) [8].

The presented high-pressure PL measurements were performed at 80 K, with the use of a diamond anvil cell (DAC). Solid argon was used as a pressure transmitting medium. The samples, cut and polished down from the substrate side to a thickness of 30 μm, were loaded into the cell along with a small ruby crystal. The R_1- line ruby luminescence was used for pressure calibration. The sample PL was excited with a Lasos DPSSL laser (wavelength of 320 nm, 3.87 eV). A maximum power of 20.4 mW on the sample surface was used, on an estimated area of 38.5 μm^2, therefore with an estimated maximum power density of around 53 kW/cm^2. Laser power was tuned by an attenuator from a maximal to minimal value of 0.4 μW (1 W/cm^2). The PL signal was detected by means of a cooled charge-coupled device (CCD) camera.

III. EXPERIMENTAL RESULTS

Figure 2 illustrates the evolution of the PL spectra for three values of LPD, under low and under high pressure (upper and lower parts of the panels, respectively). At low LPD, the PL spectra show lines that are assigned to ground states of the indirect intrawell exciton for sample A and the indirect interwell exciton for sample B. With increasing LPD, the direct exciton ground state appears. The PL peak energy of indirect excitons displays a strong blueshift with increasing LPD, related to the screening of a significant part of the built-in electric field. This blueshift can attain a magnitude of 0.5 eV, as was demonstrated in our previous paper [8]. Above a threshold magnitude of LPD, the exciton character switches from indirect to direct in both structures. In the same LPD range, we observe not only the ground state of the direct exciton (DX GS), but also the excited state (DX ES). The energy location of both DX GS and DX ES is weakly dependent on the laser power.

At first glance, the application of hydrostatic pressure to both structures results in a shift of the excitonic peaks to higher energies but it does not cause any modification of their character. Below, we discuss in more detail the changes in the PL behavior of both structures as a function of pressure and LPD.

Figure 3 shows the evolution of the exciton recombination energy versus the power density of the exciting laser for (a) sample A and (b) sample B, at different values of pressure. In general, for a fixed value of pressure, E_{PL} blueshifts markedly at low LPD, which is characteristic of IXs [8], up to threshold power densities above which the blueshift abruptly follows a much smaller slope, characteristic of DXs. Sample B exhibits a pronounced switch from DX to IX excitons (saturation of the blueshift at high LPD), whereas sample A shows only the onset of such a transition. Moreover, sample A shows a gradual increase of E_{PL} with pressure in the entire range of LPDs applied in the experiment [Fig. 4(a)]. Sample B displays a more complicated behavior: for low LPDs, E_{PL} decreases with pressure whereas for higher LPDs E_{PL} increases with pressure [Fig. 4(b)]. At some LPD value (around 0.5 kW/cm^2) E_{PL} does not change with pressure.

A closer look at the evolution of the PL energy with pressure presented in Fig. 4 reveals that for similar transition energies (E_{PL}) the pressure coefficients dE_{PL}/dp can be very different (especially at low pumping). If we compare the data from Fig. 4 with data from Ref. [25], we find that they do not follow the same dependence. This seems to be consistent with the observation from Ref. [26] that the universal dependence between E_{PL} and dE_{PL}/dp is due to the fact that the confinement energy in InGaN/GaN wells is independent of the well width L (for strong electric fields). When E_{PL} and dE_{PL}/dp are modified by screening, this independence of L is no longer valid. In our samples, even for the same total width of the well material (like for our samples A and B), the presence of barrier affects the screening and leads to different pressure coefficients for similar transition energies. When the electric field is screened (high values of LPD), the variation

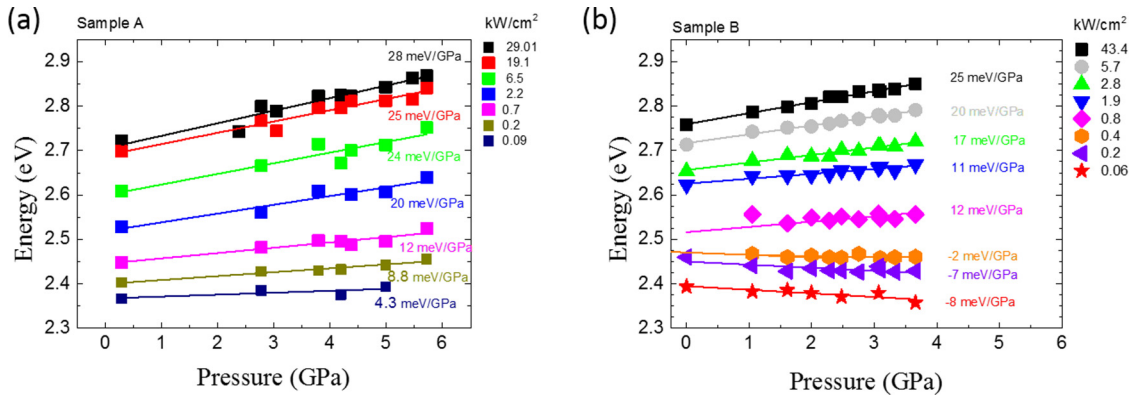

FIG. 4. Energy of excitons' ground state versus pressure for several values of power density of the exciting laser for samples A (a) and B (b). Numbers accompanying individual dependences indicate the pressure coefficients of the exciton energy dE_{PL}/dp extracted from the linear fits.

of dE_{PL}/dp as a function of E_{PL} becomes similar for both samples, and it reflects the pressure dependence of the band gap in $In_{0.17}Ga_{0.83}N$.

Inspection of Fig. 5 shows that pressure coefficients dE_{PL}/dp of both samples exhibit an approximately linear evolution with the logarithm of LPD until it approaches the threshold magnitude for switching from IX to DX. The threshold LPD for IX→DX switching is higher for sample A than for sample B, as can also be seen in Fig. 3. This is due to the more effective screening of the electric field in the double well since the barrier reduces the overlap of wave functions of electrons and holes (the charges are more separated). Thus we can expect that recombination will be reduced in sample B and more charge will accumulate in the well (for the same LPD in both samples). This seems to be confirmed by the pressure dependence of threshold LPD, shown in Fig. 6. The barriers become higher under pressure since the band gap increases faster in the $In_{0.02}Ga_{0.98}N$ barriers than in the $In_{0.17}Ga_{0.83}N$ wells. Therefore, under pressure, tunneling is further reduced in sample B. In both samples the penetration of the wave functions into the barriers should be reduced under pressure which favors the screening by free carriers, and thus also favors the creation of direct excitons.

It is worth pointing out that the observed behavior of the pressure coefficient corresponds in a qualitative way to the evolution of E_{PL} with laser excitation. In the case of IXs, efficient screening is observed, while a "saturation" of the screening characterizes the DX region. Similarly, the pressure coefficients increase in the IX region and "saturate" in the DX region.

IV. THEORY

Screening effects depend on the charge density in the quantum well n while our experimental results are expressed in terms of LPD. In order to relate those two quantities, we assume that charge generation in the well is proportional to LPD while the recombination occurs through radiative excitonic transitions and through nonradiative Shockley-Read-Hall (SRH) recombination. We neglect the contribution of Auger processes since our experiments are conducted at low temperature. Under CW illumination the generation and

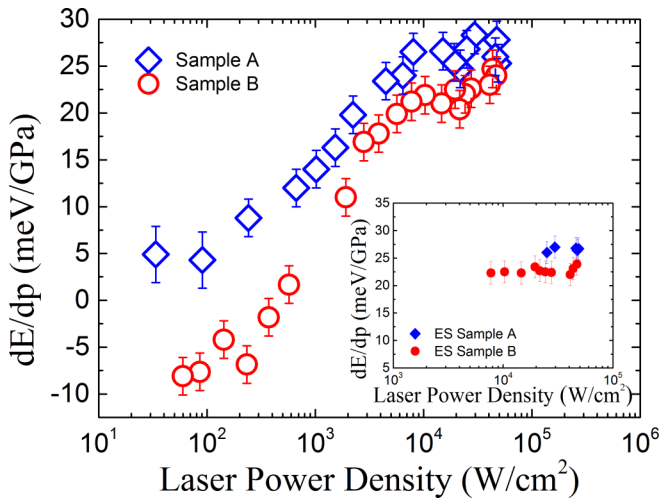

FIG. 5. Pressure coefficient dE_{PL}/dp of the PL energy of the ground exciton state for the two InGaN/GaN samples under study. The inset shows pressure coefficients of the excited exciton states.

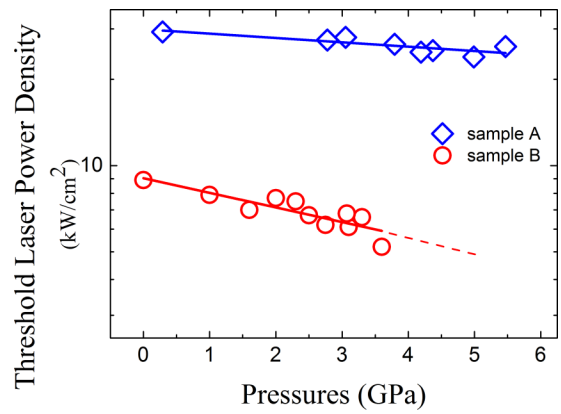

FIG. 6. Pressure dependence of the threshold power of the exciting laser for the ground exciton states switching from indirect to direct excitons.

recombination must be equal; therefore

$$CLPD = An + Bn, \tag{1}$$

where An denotes the SRH recombination and Bn is the radiative excitonic recombination (both are linear in carrier concentration n). According to theoretical predictions in Ref. [29] and the experimental results in Ref. [30] both A and B scale approximately as the square of the overlap of electron- and hole-wave functions $|\langle\varphi_e|\varphi_h\rangle|^2$. Therefore, we can write

$$\text{LPD} \propto n|\langle\varphi_e|\varphi_h\rangle|^2, \tag{2}$$

which shows that under increasing illumination of LPD the carrier concentration in the well will increase but this increase will be accompanied by the increasing recombination probability. The above proportionality will allow us to relate the theory and experiment.

We calculated the transition energies using NEXTNANO software with the material constants listed in Ref. [8]. This software solves the Schrödinger and Poisson equations in a self-consistent manner, using the effective mass approximation. The simulated structures consisted of an $In_{0.02}Ga_{0.98}N$ matrix containing either one 5.2-nm-thick $In_{0.17}Ga_{0.83}N$ QW (sample A) or two 2.6-nm-thick $In_{0.17}Ga_{0.83}N$ QWs separated by a 0.78-nm-thick $In_{0.02}Ga_{0.98}N$ barrier (sample B). Everything was modeled fully strained on the GaN substrate.

The photogeneration of carriers was simulated by assuming an injection of electrons that decreases exponentially from the semiconductor surface, with the exponential decay constant being the absorption coefficient for the PL excitation laser wavelength ($\alpha = 1.2 \times 10^5 \text{cm}^{-1}$ [31]). We refer to this density as the "injected carrier density" (N). We assume that this quantity is proportional to the LPD. However, the screening of the field in the QW is governed by the carrier concentration in the well n. For a given N we calculate n and the recombination rate $|\langle\varphi_e|\varphi_h\rangle|^2$.

The overlap matrix element squared is shown in Fig. 7. For low N the recombination rate is 10 times higher for the single QW than for the double QW, which shows that the barrier in the middle of the well plays an important role in reducing the overlap in sample B. This means that the radiative lifetime will be significantly longer in sample B, which should lead to higher density of electrons in the well under optical pumping, and more efficient screening of the electric field.

We can plot the theoretical transition energies as a function of $n|\langle\varphi_e|\varphi_h\rangle|^2$ which should be proportional to LPD [see Eq. (2)]. Since we do not know the proportionality constant, we treat it as a fitting parameter; i.e., we shift the theoretical curves along the horizontal axis (in logarithmic coordinates) so as to approach the experimental points. The result is shown in Fig. 8 where the upper scale shows the LPD and the lower scale represents $n|\langle\varphi_e|\varphi_h\rangle|^2$. The agreement is fairly good, taking into account all the approximations of the calculation.

The transition energy at high excitation power (high injected carrier density) is mostly determined by the $In_{0.17}Ga_{0.83}N$ band gap, since the internal electric field is almost fully screened. On the contrary, at low excitation power, the transition energy is given by the internal electric field induced by spontaneous and piezoelectric polarization.

A closer inspection of Fig. 8 shows that for a given $n|\langle\varphi_e|\varphi_h\rangle|^2$ the corresponding LPD is higher for sample B than

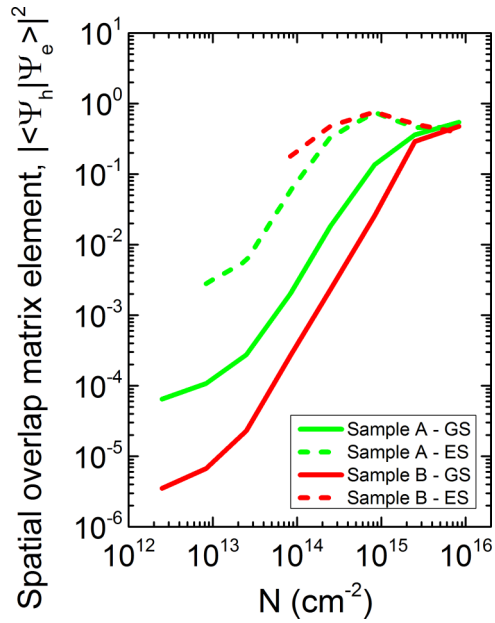

FIG. 7. Square of the overlap matrix element as a function of injected charge density N for ground and excited state transitions in single QW (sample A) and in double QW (sample B). Since N decays exponentially in the sample, we represent it by its value at the sample surface.

for sample A. The proportionality constant between LPD and $n|\langle\varphi_e|\varphi_h\rangle|^2$ depends on the sum of nonradiative and radiative recombination rates, as follows from Eqs. (1) and (2). The presence of the thin barrier in sample B could give rise to an increased nonradiative recombination rate. However, the main difference between the two samples (leading to more effective screening in sample B) seems to be related to different wave function overlaps, as shown in Fig. 7.

The calculated transition energies can also be plotted as a function of the electric field in the well, as depicted in Fig. 9. For this representation, we took the calculated value of the

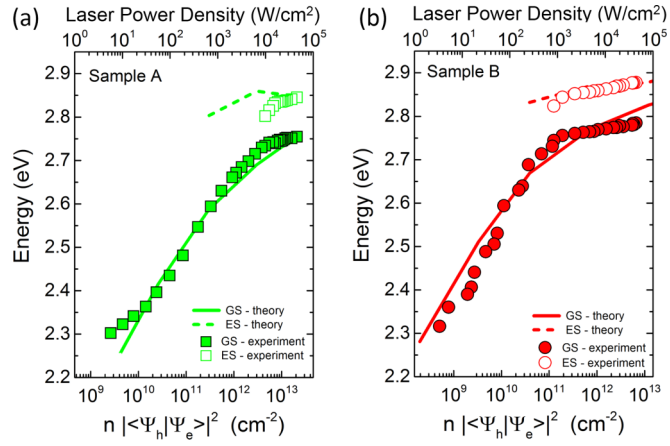

FIG. 8. Comparison of experimental transition energies (points) with theory (solid lines) for two samples: (a) sample A and (b) sample B. The theoretical curves were plotted as a function of $n|\langle\varphi_e|\varphi_h\rangle|^2$ (lower scale) and the experimental points as a function of LPD (upper scale).

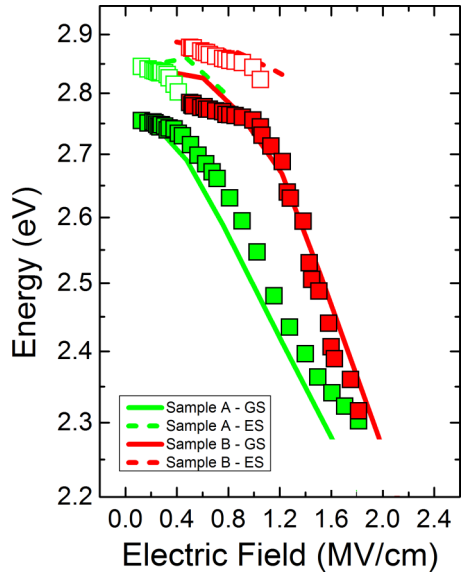

FIG. 9. Transition energies plotted as a function of average electric field in the well. Curves are theoretical.

field in the middle of the well (sample A) or the average of the electric fields in the two wells (sample B). The experimental data are superimposed in this plot.

Now we turn to theoretical determination of pressure coefficients for the transition energies. Since NEXTNANO does not describe pressure effects we performed a simplified analysis based on the case of uniform fields in the well (which is a rough approximation in the presence of screening; see Fig. 1).

The transition energies in the $In_xGa_{1-x}N/GaN$ quantum well can be written as

$$E_x = E_g^x + E_{\text{conf}}^e + E_{\text{conf}}^h - eLF_{\text{int}} - E_{\text{exc}}, \tag{3}$$

where E_g^x is the band gap of the well material, L is the well width, F_{int} is the electric field in the well, E_{exc} is the binding energy of exciton, and E_{conf}^e and E_{conf}^h are the confinement energies, measured from the lower edge of the conduction band in the well for electrons and from the higher edge of the valence band in the well for holes, respectively. This equation does not account for the presence of free carriers in the well; i.e., screening is neglected. In the following we shall assume that screening will reduce the average field in the well but we shall still use the above equation.

In Eq. (3), E_g^x depends on pressure but does not change with the electric field. All other terms depend on F_{int}, and we can assume that their dependence on pressure is due to the pressure dependence of F_{int}. All other quantities that depend on pressure such as the effective masses, exciton binding energy, or well depth changes, are expected to have a much weaker effect on the transition energies. Therefore, we can write

$$\frac{dE^x}{dp} = \frac{dE_g^x}{dp} + \frac{dE^x}{dF_{\text{int}}}\frac{dF_{\text{int}}}{dp}. \tag{4}$$

The pressure variation of the electric field has been calculated in Ref. [26] as

$$F_{\text{int}}(p, x) = [15 + 0.64p]x, \tag{5}$$

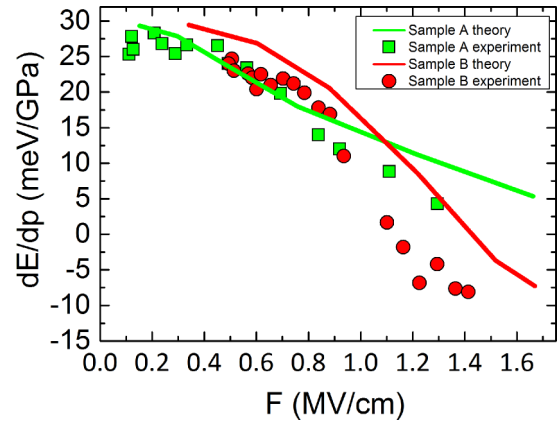

FIG. 10. Experimental pressure coefficients as a function of the average electric field in the well. Green (red) symbols correspond to sample A (sample B). Lines are theoretical.

where the pressure is in GPa and the field in MV/cm. This is the maximum built-in field in the $In_xGa_{1-x}N/GaN$ well, but it will be reduced by residual carriers or by free carriers due to optical or electrical pumping. If we assume, for simplicity, that the screening reduces this field by a factor α, we obtain (for $x = 0.17$)

$$\frac{dF_{\text{int}}}{dp} = 0.1088\alpha = 0.1088\frac{F_{\text{int}}(0, x)}{2.55}, \tag{6}$$

where $F_{\text{int}}(0, x)$ is the field at ambient pressure. This is due to the fact that the factor α reduces both the field at zero pressure and the term proportional to pressure in Eq. (5) ($15 \times 0.17 = 2.55$).

Equations (4) and (6) allow us to determine the pressure coefficients of the transition energy if we know the electric field dependence of this transition. We differentiate the theoretical curves shown in Fig. 9 with respect to the electric field in the well. We set $\frac{dE_g^x}{dp}$ for $x = 0.17$ as 30 meV/GPa [32]. Finally, using Eqs. (4) and (6) we obtain the pressure coefficients of the corresponding transitions, shown in Fig. 10 together with experimental data. For the experimental data, we use the same correspondence between LPD and electric field as determined from the fit of transition energies. The agreement is only qualitative but we note that the negative pressure coefficients observed for the double QW at high electric fields (low injection) are also described by the theory. This follows from the fact that the barrier in the middle of the double QW reduces the wave function overlap (i.e., the recombination rate) so that the charge density is higher in this well. This leads to higher transition energies in the double QW but also to higher (in absolute value) negative derivative $\frac{dE^x}{dF_{\text{int}}}$ in Eq. (4) (see Fig. 9), which explains negative pressure coefficients for the double QW at low LPD.

V. SUMMARY AND CONCLUSIONS

We analyzed the transition energies (obtained from photoluminescence spectra) in two InGaN/GaN quantum well samples as a function of excitation power and hydrostatic pressure. We found that both E_{PL} and dE_{PL}/dp reveal a strong variation in the range of LPD corresponding to indirect

excitons, while for direct excitons this variation was much weaker. The presence of a thin barrier in the middle of the quantum well reduced the recombination and improved the screening (compared to the well without barrier). The saturation of both E_{PL} and dE_{PL}/dp occurred at lower LPD in the double QW with a 0.78-nm-wide barrier. This double QW revealed negative pressure coefficients for low pumping levels while the single QW had positive dE_{PL}/dp in the whole range of LPDs. We observed therefore different pressure coefficients for the two samples even when the transition energies were similar. This is related to the fact that screening changes in the presence of the barrier. It also depends on the well width L; therefore the confinement energies are no longer independent of L. All this implies that the "universal" relationship between E_{PL} and dE_{PL}/dp observed in Ref. [25] does not hold for samples modified by screening.

The experimental data are in qualitative agreement with calculations. We believe that the presented results demonstrate the usefulness of hydrostatic pressure as a tool to study an internal electric field and its screening in polar semiconductor heterostructures.

ACKNOWLEDGMENT

This work was supported by the Polish National Science Center, Grants No. 2013/11/B/ST3/04263 and No. 2015/17/B/ST7/04091.

[1] S. Nakamura and S. F. Chichibu, *Introduction to Nitride Semiconductor Blue Lasers and Light Emitting Diodes* (Taylor & Francis, London, 2000).
[2] S. Nakamura, T. Mukai, and M. Senoh, Appl. Phys. Lett. **64**, 1687 (1994).
[3] S. Nakamura, M. Senoh, S.-i. Nagahama, N. Iwasa, T. Yamada, T. Matsushita, H. Kiyoku, and Y. Sugimoto, Jpn. J. Appl. Phys. **35**, L74 (1996).
[4] M. R. Krames, O. B. Shchekin, R. Mueller-Mach, G. O. Mueller, L. Zhou, G. Harbers, and M. G. Craford, J. Disp. Technol. **3**, 160 (2007).
[5] S. Pimputkar, J. S. Speck, S. P. DenBaars, and S. Nakamura, Nat. Photon. **3**, 180 (2009).
[6] P. Lefebvre, S. Kalliakos, T. Bretagnon, P. Valvin, T. Taliercio, B. Gil, N. Grandjean, and J. Massies, Phys. Rev. B **69**, 035307 (2004).
[7] O. Ambacher, J. Majewski, C. Miskys, A. Link, M. Hermann, M. Eickhoff, M. Stutzmann, F. Bernardini, V. Fiorentini, V. Tilak, B. Schaff, and L. F. Eastman, J. Phys.: Condens. Matter **14**, 3399 (2002).
[8] T. Suski, G. Staszczak, K. P. Korona, P. Lefebvre, E. Monroy, P. A. Drozdz, G. Muzioł, C. Skierbiszewski, M. Kulczykowski, M. Matuszewski, E. Grzanka, S. Grzanka, K. Pieniak, K. Gibasiewicz, A. Khachapuridze, J. Smalc-Koziorowska, L. Marona, and P. Perlin, Phys. Rev. B **98**, 165302 (2018).
[9] Y. J. Chen, E. S. Koteles, B. S. Elman, and C. A. Armiento, Phys. Rev. B **36**, 4562 (1987).
[10] F. Bernardini, V. Fiorentini, and D. Vanderbilt, Phys. Rev. B **56**, R10024 (1997).
[11] T. Takeuchi, C. Wetzel, S. Yamaguchi, H. Sakai, H. Amano, I. Akasaki, Y. Kaneko, S. Nakagawa, Y. Yamaoka, and N. Yamada, Appl. Phys. Lett. **73**, 1691 (1998).
[12] S. Charbonneau, M. L. W. Thewalt, E. S. Koteles, and B. Elman, Phys. Rev. B **38**, 6287 (1988).
[13] A. Moskalenko and D. Snoke, *Bose-Einstein Condensation of Excitons and Biexcitons* (Cambridge University, Cambridge, UK, 2005).
[14] L. V. Butov, A. L. Ivanov, A. Imamoglu, P. B. Littlewood, A. A. Shashkin, V. T. Dolgopolov, K. L. Campman, and A. C. Gossard, Phys. Rev. Lett. **86**, 5608 (2001).
[15] G. Grosso, J. Graves, A. T. Hammack, A. A. High, L. V. Butov, M. Hanson, and A. C. Gossard, Nat. Photon. **3**, 577 (2009).
[16] A. A. High, J. R. Leonard, A. T. Hammack, M. M. Fogler, L. V. Butov, A. V. Kavokin, K. L. Campman, and A. C. Gossard, Nature (London, U. K.) **483**, 584 (2012).
[17] A. G. Winbow, A. T. Hammack, L. V. Butov, and A. C. Gossard, Nano Lett. **7**, 1349 (2007).
[18] Y. Y. Kuznetsova, M. Remeika, A. A. High, A. T. Hammack, L.V. Butov, M. Hanson, and A. C. Gossard, Opt. Lett. **35**, 1587 (2010).
[19] P. Andreakou, S. V. Poltavtsev, J. R. Leonard, E. V. Calman, M. Remeika, Y. Y. Kuznetsova, L. V. Butov, J. Wilkes, M. Hanson, and A. C. Gossard, Appl. Phys. Lett. **104**, 091101 (2014).
[20] F. Fedichkin, P. Andreakou, B. Jouault, M. Vladimirova, T. Guillet, C. Brimont, P. Valvin, T. Bretagnon, A. Dussaigne, N. Grandjean, and P. Lefebvre, Phys. Rev. B **91**, 205424 (2015).
[21] F. Fedichkin, T. Guillet, P. Valvin, B. Jouault, C. Brimont, T. Bretagnon, L. Lahourcade, N. Grandjean, P. Lefebvre, and M. Vladimirova, Phys. Rev. Appl. **6**, 014011 (2016).
[22] M. Dvorak, S.-H. Wei, and Z. Wu, Phys. Rev. Lett. **110**, 016402 (2013).
[23] C. Netzel, V. Hoffmann, T. Wernicke, A. Knauer, M. Weyers, M. Kneissl, and N. Szabo, J. Appl. Phys. **107**, 033510 (2010).
[24] P. Perlin, I. Gorczyca, T. Suski, P. Wisniewski, S. Lepkowski, N. E. Christensen, A. Svane, M. Hansen, S. P. DenBaars, B. Damilano, N. Grandjean, and J. Massies, Phys. Rev. B **64**, 115319 (2001).
[25] T. Suski, S. P. Łepkowski, G. Staszczak, R. Czernecki, P. Perlin, and W. Bardyszewski, J. Appl. Phys. **112**, 053509 (2012).
[26] W. Trzeciakowski, A. Bercha, and M. Gładysiewicz-Kudrawiec, J. Appl. Phys. **124**, 205701 (2018).
[27] T. Suski, H. Teisseyre, S. P. Lepkowski, P. Perlin, T. Kitamura, Y. Ishida, H. Okumura, and S. F. Chichibu, Appl. Phys. Lett. **81**, 232 (2002).
[28] P. Perlin, W. Trzeciakowski, E. Litwin-Staszewska, J. Muszalski, and M. Micovic, Semicond. Sci. Technol. **9**, 2239 (1994).
[29] E. Kioupakis, Q. Yan, and C. G. Van de Walle, Appl. Phys. Lett. **101**, 231107 (2012).

[30] A. David, C. A. Hurni, N. G. Young, and M. D. Craven, Appl. Phys. Lett. **111**, 233501 (2017).

[31] J. F. Muth, J. H. Lee, I. K. Shmagin, R. M. Kolbas, H. C. Casey, Jr., B. P. Keller, U. K. Mishra, and S. P. DenBaars, Appl. Phys. Lett. **71**, 2572 (1997).

[32] G. Franssen, I. Gorczyca, T. Suski, A. Kamińska, J. Pereiro, E. Muñoz, E. Iliopoulos, A. Georgakilas, S. B. Che, Y. Ishitani, A. Yoshikawa, N. E. Christensen, and A. Svane, J. Appl. Phys. **103**, 033514 (2008).